ACS OMEGA

http://pubs.acs.org/journal/acsodf

Article

Role of FeS Catalyst in the Hydromodification of Lignite in a Subcritical Water−CO System

Yuqiong Zhao,* Shouqi He, Qingxiang Guo, Guoqiang Li, Liping Wang, Yunbo Liu, and Yongfa Zhang*

Cite This: *ACS Omega* 2021, 6, 21160−21168

Read Online

ACCESS | Metrics & More | Article Recommendations

ABSTRACT: The impacts of FeS catalysts on the hydromodification and structural evolution of lignite were investigated using Fourier transform infrared spectroscopy, nuclear magnetic resonance, and X-ray photoelectron spectroscopy. The results indicate that the caking property of lignite can be significantly improved in the presence of the FeS catalyst. When 6.0 wt % FeS was added, the maximum caking index (G_{RI}) of modified coal reached 95. During the hydromodification, FeS has little effect on the intrinsic water gas shift reaction, but it can increase the CO conversion by promoting the decomposition and hydrogenation of coal so that more active hydrogen is generated and introduced into modified coal. FeS is conducive to the rupture of distal aliphatic groups in the extractible solutes, which promotes the entrance of hydrogen into the aromatic nucleus (H_{ar}) and α positions (H_α) of asphaltenes and β positions (H_β) of preasphaltenes. After the catalytic hydromodification, the longer side chains or bridge bonds break and are hydrogenated to form the aliphatic structures with a shorter chain or a higher branched degree. Meanwhile, more oxygen-containing functional groups were removed along with the reduction of volatiles in the modified coal. The synergistic effect of FeS on these factors is favorable for the generation of plastic materials, which contributes to the development of the caking property of lignite.

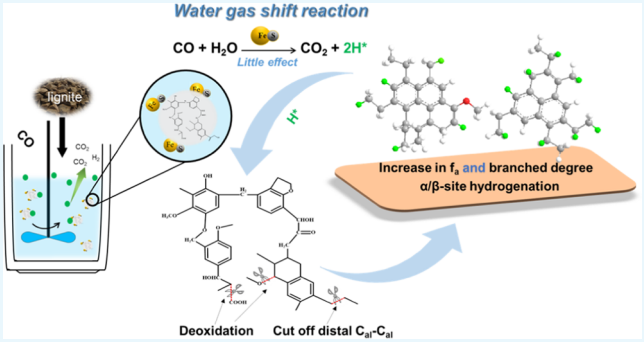

1. INTRODUCTION

China has enormous deposits of lignite with total reserves estimated to be approximately 130 billion tons, and most of the lignite has lower ash content and is also cheap.[1] However, its utilization has been limited because of the high content of oxygen and moisture, as well as the noncaking characteristic. If lignite could be converted into caking coal, it would improve the utilization of lignite and open coking coal resources. To develop the caking propensity of noncaking coal, various coal modification techniques have been attempted, and these mainly include thermal treatment at low temperature, hydrothermal treatment, and hydrogenation modification.[2−13]

Thermal and hydrothermal treatments have been historically used for modifying coal. In these processes, oxygen-containing functional groups are removed, and the combination of intramolecular and intermolecular interactions in coal is weakened. The mechanisms for how these two methods increase the caking characteristic of coal are as follows: (1) deoxygenation inhibits the cross-linking reactions and reduces the hydrogen consumption during pyrolysis and (2) the rupture of noncovalent and weak covalent bonds increases the amount of extractible materials that is related to the caking characteristic of coal. Unfortunately, the above-mentioned methods have limited success. Shui et al.[5] reported that hydrothermal treatment at 300 °C with CaO increased the caking index (G_{RI}) of a mixture of Shengfu coal and rich coal from 46.7 to only 54.0. In contrast, hydrogenation modification is an effective process for improving the caking characteristic of low-rank coal. Wang et al.[14] observed that the hydromodification of Shenhua coal in the tetralin-H_2 system promoted the generation of some active components with medium molecular structures and increased the degree of order in the coal, which improved the G_{RI} from 0 to 60 at a temperature of 350 °C. Our previous work[3] involved the hydromodification of lignite in a subcritical water−CO system and exhibited better results than those of Wang et al. When FeS was used as a catalyst, the G_{RI} of modified coal could reach or exceed the value of 90 (the G_{RI} of lignite is 0). However, the role of FeS in hydromodification is not well understood.

In fact, numerous studies have focused on studying the role of iron-based catalysts in the hydrogenation of coal.[15−21] For the hydropyrolysis of coal, researchers found that the catalytic

Received: June 14, 2021
Accepted: July 23, 2021
Published: August 5, 2021

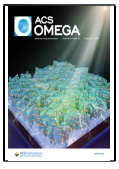

Table 1. Proximate and Ultimate Analyses of Lignite

	proximate analysis (wt %), ad				ultimate analysis (wt %), daf					
samples	M	A	V	FC	C	H	O[a]	N	S	G_{RI}
Inner Mongolian lignite	12.22	9.22	39.74	38.82	79.10	6.26	12.65	1.52	0.47	0

[a]By difference.

activity of iron on cracking was higher than that on hydrogenation, which changes the composition of tar and makes it lighter.[16] In the coal liquefaction process, the conventional theory suggested that iron-based catalysts can split molecular hydrogen into tetralin and then catalyze the fast dehydrogenation of tetralin to release hydrogen for coal hydrogenation.[17,18] However, several researchers reported that catalysts directly promote the transfer of hydrogen from molecular hydrogen to coal rather than through tetralin.[19,20] Li et al.[21] revealed that iron-based catalysts mainly promoted coal pyrolysis and the formation of activated hydrogen to accelerate the secondary distribution of H in the reaction. Niu et al.[22] reported that iron-based catalysts can directly promote the hydrogen transfer and exchange between coal and the solvent, whereas the α-radical of tetralin acts as an important intermediate.

Obviously, the above-mentioned theories are not applicable for understanding the role of FeS in hydromodification in a subcritical water−CO system because of the differences in the reaction systems and target products. In a subcritical water−CO system, the water gas shift reaction (WGSR, $H_2O + CO \rightarrow CO_2 + H_2$) is responsible for providing active hydrogen.[23−27] Meanwhile, coal in hot water would decompose and the free radicals from coal decomposition could react with active hydrogen to achieve hydrogenation. In other words, water, CO, and coal are involved in the process and can interact with each other. Even more important is that these reactions may lead to the coal's structural evolution, which corresponds to changes in the caking characteristic of lignite. Therefore, the effects of FeS on multiple reactions and coal's structural characteristics need a deeper understanding.

In this paper, FTIR, ^{1}H NMR, ^{13}C NMR, and XPS were used to study the impact of FeS on hydromodification and structural evolution of lignite in a subcritical water−CO system. Particular attention was paid to the relationship between these effects and the caking properties of modified coal.

2. EXPERIMENTAL SECTION

2.1. Materials. An Inner Mongolian lignite was used in this study. The lignite was ground and sieved to a particle size of less than 100 mesh and dried for 10 h under vacuum at 100 °C before hydromodification.[24] The properties of the coal samples are presented in Table 1. Water was used as the solvent, and the reaction atmosphere was CO or N_2 (purity >99.9%).

2.2. Hydromodification Experiments. Coal hydromodification was carried out in a 300 mL autoclave with a magnetic stirrer.[3] First, 30 g of lignite, 30 g of water, and 0.0−8.0 wt % (i.e., 0.0, 1.0, 2.0, 4.0, 6.0, 8.0, 10.0 wt %) FeS of lignite were added to the autoclave. Carbon monoxide was used to flush out the residual air in the reactor. Gas flushing was performed two or three times to ensure there was no residual air in the reactor. The autoclave reactor was pressurized with CO to 4.0 MPa (G) at room temperature. The autoclave was then heated to 340 °C, which is the optimized reaction temperature,[3] and the temperature was maintained for 30 min. The reactor was later cooled to room temperature. The gas product was carefully released and analyzed using a GC-950 gas chromatograph (Shanghai Linghua Co., Ltd., China) and a VARIAN CP-3800 gas chromatograph. The solid product was filtered to remove excess water and dried overnight under a vacuum at 80 °C. Finally, the modified coals were obtained. Herein, the modified coals are denoted as Mc, where c represents the content of FeS. The caking index of modified coals was measured according to the national standard of China GB/T5447-2014 ("determination of the caking index of bituminous coal").

2.3. CO Conversion Calculations. CO conversion X_{CO} is typically used to represent the conversion of WGSR. On the basis of our previous study,[3] X_{CO} for every run was calculated using eq 1.

$$X_{CO} = 1 - (P' y'_{CO} Z_{CO})/(Z'_{CO} P y_{CO}) \quad (1)$$

where P and P' are the pressures of gases before and after the reaction, respectively, y_{CO} and y_{CO}' are the volume fractions of CO before and after reaction, respectively, and Z_{co} and Z_{co}' are compressibility factors of CO before and after reaction, respectively.

2.4. Extraction. Raw coal and modified coals were extracted using n-hexane, benzene, and tetrahydrofuran (THF) sequentially using a Soxhlet extractor. Approximately 15.0 g of dried modified coal and n-hexane were charged into a Soxhlet apparatus and extracted until the solvent became colorless. After that, the residue was dried for 12 h under vacuum at 80 °C, and then it was extracted again following the same procedure with benzene and THF as solvents. The *n*-hexane soluble, *n*-hexane insoluble/benzene soluble, and benzene insoluble/THF soluble were defined as oil, asphaltenes (AS), and preasphaltenes (PS), respectively. The total extractible material (oil + AS + PS) is denoted as TT. The Soxhlet extraction yield was calculated based on the weight of the residue.[3]

2.5. Sample Characterization. Carbon distribution of coal samples and hydrogen distribution of extractible constituents were performed by ^{13}C NMR and ^{1}H NMR spectra (Bruker AVANCE III 600M NMR spectrometer). Oil and AS were dissolved in deuterated chloroform ($CDCl_3$), and PS was dissolved in dimethyl sulfoxide-D_6 ($(CD_3)_2SO$). Tetramethylsilane (TMS) was used as an internal reference.

FTIR analyses of raw coal and the hydrothermally treated coals with or without the addition of FeS were conducted on a Nicolet iS10 Fourier transform infrared spectrometer. For the spectroscopic analysis, 1 mg of the sample was mixed with 100 mg of KBr and pressed to form a pellet. The scanning range was from 4000 to 400 cm^{-1}, and a total of 32 scans were performed with a spectral resolution of 4 cm^{-1}.

X-ray photoelectron spectra were determined using an ESCALAB250 spectrometer using Al K non-monochromatic radiation. The X-ray source was operated at 200 W and 60 eV pass energy was used for narrow scans. C 1s (284.8eV) was

https://doi.org/10.1021/acsomega.1c03120
ACS Omega 2021, 6, 21160−21168

used for charge calibration and the curve-fitting analysis of the XPS spectrum was performed using the curve-fitting function.

3. RESULTS AND DISCUSSION

3.1. Effect of FeS on the Caking Property of Modified Coals and the Composition of Gas Products.

Figure 1

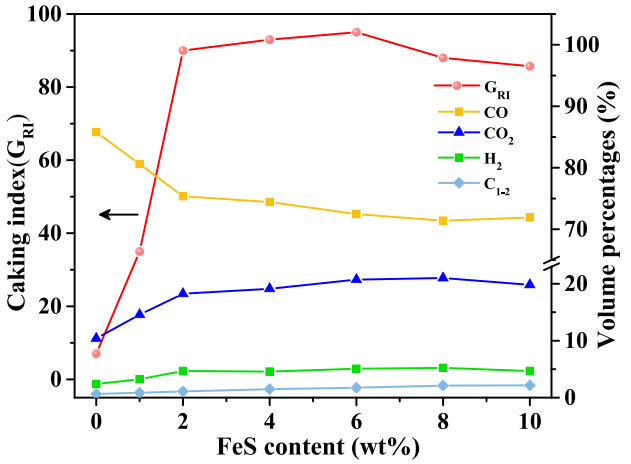

Figure 1. Influence of FeS on the caking index of modified coal and composition of gas products.

shows the caking index (G_{RI}) of modified coal as a function of FeS loading (from 0 to 10.0 wt %). Compared to hydromodification without a catalyst, the addition of FeS can significantly improve the caking of modified coal, suggesting that FeS plays an important role in promoting coal hydromodification in a subcritical water−CO system. The value of G_{RI} increases with an increase in the content of FeS, reaching a maximum (95.0) at 6.0 wt % FeS, and then decreases with any additional increase in the catalyst's content. The higher catalytic activities of catalysts with high FeS content may be attributed to an increased number of total active sites, which is beneficial for the modulation of coal structure. Further addition of FeS is detrimental to the development of the caking property, and the G_{RI} of the modified coal decreased to 85.7 at an FeS loading of 10.0 wt %. This is because the catalyst would enter into modified coals after hydromodification and the excessive addition of FeS could increase the ash content in the modified coals, thus leading to a continual decrease in the caking index.

The influence of FeS content on the composition of gas products during coal hydromodification is also shown in Figure 1. Before the coal hydromodification, the reactor was filled with 100% CO. After the reaction, the CO content initially declines rapidly and then shows a slight decrease when the FeS loading was increased from 0 to 10.0 wt %. This phenomenon is contrary to the pattern of change in the CO_2 content. This indicates that FeS promotes the conversion of CO to CO_2. Previous studies have found that the active hydrogen produced from WGSR provides an important hydrogen source for coal hydromodification.[3] Therefore, although the stoichiometric numbers of CO_2 and H_2 are equal in the WGSR ($H_2O + CO \rightarrow CO_2 + H_2$), the content of H_2 changes little compared to the CO_2 content and only increases from 2.39 to 4.68%.

3.2. Effect of FeS on the Water Gas Shift Reaction during Coal Hydromodification.

To further understand the effects of FeS on the WGSR, the conversions of CO (X_{CO}) for every run were calculated based on eq 1. The parameters and calculation results are presented in Table 2. It can be seen that X_{CO} increases with the increase in FeS loading and then gradually decreases, which is similar to the variation trend of G_{RI}. This phenomenon suggests that the conversion of CO is closely related to the development of caking properties in a subcritical water−CO system. The larger value of X_{CO} indicates a more abundant generation of active hydrogen in the reaction system, which provides the preconditions for the generation of caking components.[28] Indeed, there are two reasons for the improvement of X_{CO}. First, FeS catalyzes the WGSR and accelerates the kinetic reaction rate of WGS. Second, FeS promotes coal hydrogenation and increases active hydrogen consumption so that the chemical equilibrium favors the forward reaction of WGS and increases X_{CO}. To explore which reason dominates the conversion of CO and which does not, the effect of FeS on X_{CO} was measured without adding coal, while keeping all other reaction parameters unchanged (see Table 2). X_{CO} was found to be 2.61% with the addition of 6.0 wt % FeS, which indicates an increase of only 0.39% as compared to 2.22% observed without the addition of FeS. It reveals that the addition of FeS has little effect on the WGSR, whereas FeS improves the CO conversion mainly by enhancing coal hydrogenation to promote the forward reaction of WGS. It can also be observed that the final pressures (P') reached 4.5 MPa without coal and was much higher than that with coal; this can be ascribed to only a small consumption of active hydrogen, which increased the pressure.

Figure 2 presents the influence of FeS content on the composition of gas products with/without adding coal. In the absence of coal, the composition of H_2 and CO_2 in the product gas was basically the same whether the catalyst was added or

Table 2. Parameters and CO Conversions for Every Run

FeS (wt %)	P_{co} (MPa(A))	$P_{r,co}$	Z_{co}	P' (MPa)	y_{co}' (%)	P_{co}' (MPa)	$P_{r,co}'$	Z_{co}'	X_{co} (%)
0.0	4.1	1.17	0.99	3.50	85.79	3.00	0.86	0.985	26.39
1.0	4.1	1.17	0.99	3.60	80.61	2.90	0.83	0.985	28.86
2.0	4.1	1.17	0.99	3.60	75.37	2.71	0.78	0.983	33.35
4.0	4.1	1.17	0.99	3.50	74.43	2.61	0.74	0.981	35.88
6.0	4.1	1.17	0.99	3.40	72.47	2.46	0.70	0.980	39.29
8.0	4.1	1.17	0.99	3.60	71.39	2.57	0.73	0.981	36.74
10.0	4.1	1.17	0.99	3.60	71.91	2.63	0.74	0.981	36.28
0.0[a]	4.1	1.17	0.99	4.45	89.81	4.00	1.14	0.987	2.22
6.0[a]	4.1	1.17	0.99	4.50	88.46	3.98	1.14	0.987	2.61

[a]Without coal. Critical temperature T_c = 132.9 K, critical pressure P_c = 3.5 MPa, reduced temperature $T_{r,co} = T_{r,co}' = 298.15/132.9 = 2.24$, $Z_{co} \propto (T_{r,co}, P_{r,co})$, $Z_{co}' \propto (T_{r,co}', P_{r,co}')$.

https://doi.org/10.1021/acsomega.1c03120
ACS Omega 2021, 6, 21160−21168

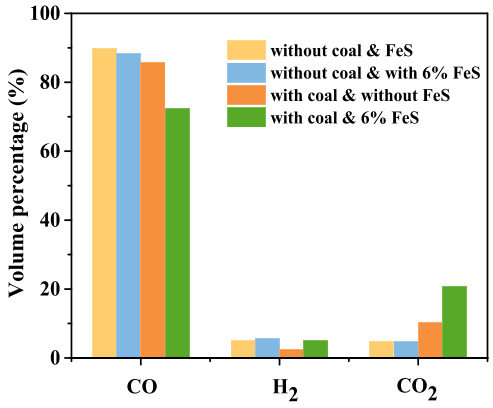

Figure 2. Influence of FeS content on the composition of gas products with/without adding coal.

not, while the content of H_2 became lower than the content of CO_2 after the addition of coal. Furthermore, the gap between the contents of H_2 and CO_2 increased with the conversion of CO in the presence of FeS. This once again confirmed that FeS improve the CO conversion mainly by promoting the hydrogenation of coal.

Additionally, although the X_{CO} value was lower with an undoped FeS catalyst during the hydromodification of coal, the value still reached 26.39%, indicating that a certain amount of active hydrogen was supplied to the system. However, the corresponding G_{RI} was only 6. This suggests that the generation of active hydrogen is not the only factor that affects the hydromodification. The effect of FeS on other reactions could also influence the caking characteristic of modified coal.

3.3. Effect of FeS on the Structure Evolution of Lignite in Subcritical Water. To explore the effect of FeS on the structure evolution of lignite in subcritical water, N_2 was used instead of CO and the amount of catalyst used varied between 0 and 6.0 wt % FeS of coal. Figure 3 presents the FTIR spectra of raw coal and a subcritical water treated coals with and without FeS addition. The peaks at 2920, 2850, and 1450 cm^{-1} were assigned to aliphatic C−H vibration

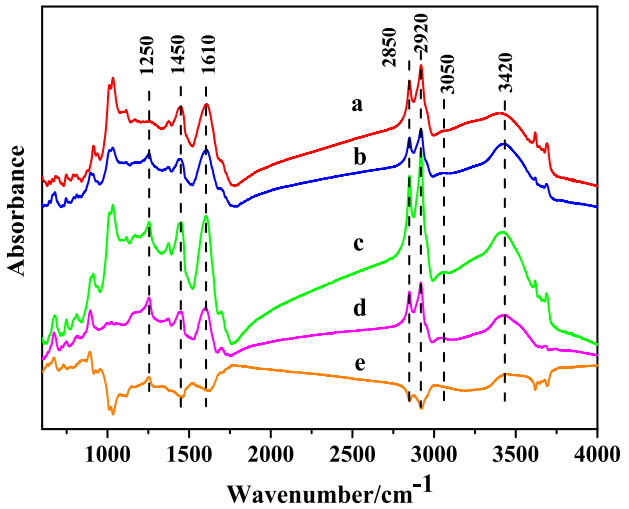

Figure 3. FTIR spectra of raw coal (a), subcritical-water-treated coal without catalyst (b), subcritical-water-treated coal with 6% FeS (c), the differences c−a (d) and b−a (e).

absorption[29] and showed a decrease in the intensity for subcritical-water-treated coal without FeS (see Figure 3e). This indicates that some weak C_{al}−H bonds of lignite could break in subcritical water without the catalyst. However, the difference in spectrum d shows that subcritical water treated coal with FeS induced an increase in aliphatic groups. Moreover, the peaks at 3050 and 700−900 cm^{-1}, corresponding to the vibration of aromatic C−H and aromatic substitution C−H bonds, progressively became visible. This reveals that the extra hydrogen was incorporated in the structure of coal with the addition of FeS. Siskin et al.[30] pointed out that water can transfer hydrogen to organic free radicals during hydrous pyrolysis. In this case, it can be inferred that the presence of FeS in a subcritical water−N_2 system may enhance the hydrolysis reaction and hydrogen transfer, thus more hydrogen is introduced into a subcritical water treated coal. As a consequence, the difference in spectrum d showed an increase in the self-associated OH hydrogen bonds, hydrogen-bonded carbonyl group, and the phenol and alcoholate types of C−O bonds; this is because of the increase in OH coming from the hydrated reaction that is catalyzed by FeS, as indicated by the increase in the intensity of bands near 3420, 1610, and 1250 cm^{-1}.[5]

Figure 4 displays the reaction pressure and temperature when the lignite is heated in the water−N_2 system with and

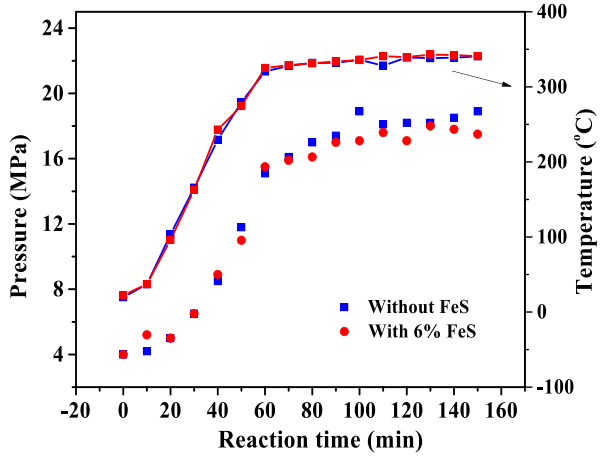

Figure 4. Pressure−time and temperature−time curves during the heating process.

without FeS addition. In both cases, there was little difference in temperature, while the pressures were basically the same below the temperature of 300 °C. However, as the temperature increased, the pressure with FeS became lower than that without FeS, which suggests that some components may have been introduced into a subcritical-water-treated coal and liquid phase, leading to a decrease in the quantity of gas. As indicated by the results presented in Table 3, the H_2 content of gas products was lower in the presence of FeS. This observation

Table 3. Composition of Gas Products under Subcritical Water−N_2 System

	composition of gas products (vol %)		
FeS content (wt %)	CO_2	CO	H_2
0.0	2.05	0.04	0.34
6.0	2.15	0.15	0.25

https://doi.org/10.1021/acsomega.1c03120
ACS Omega 2021, 6, 21160−21168

Table 4. Ultimate Analysis and Free Hydrogen Contents of Raw Coal and Modified Coals

	ultimate analysis (wt %), daf							
sample	C	H	O[a]	N	S_t	content of free hydrogen	V_{daf} (wt %)	G_{RI}
raw coal	79.10	6.26	12.65	1.52	0.47	4.68	50.59	0
M_0	79.63	6.29	12.00	1.59	0.49	4.79	47.59	6
M_6	81.55	6.45	8.75	1.52	1.73	5.36	45.33	95

[a]By difference.

can probably be explained by the catalytic effect of FeS on hydrolysis and coal hydrogenation. FeS promotes the interplay between coal and water so that a part of OH associates with the functional groups of coal, as described in Figure 3c. As a result, the hydrogen that dissociated from water is partly stabilized in the coal and liquid phase under the catalytic effect of FeS, which decreases the content of H_2 in the gas products. This observation also coincides with the results obtained from the FTIR analysis in the current work.

3.4. Effect of FeS on the Coal Hydrogenation during Coal Hydromodification. The free hydrogen content of coal is considered to be one of the most relevant factors to affect the caking of coal.[31] The free hydrogen content is calculated according to the empirical correlation given by eq 2.[32]

$$\text{free hydrogen content} = H_{daf} - O_{daf}/8 \quad (2)$$

The ultimate analysis of modified coals obtained with and without FeS loading was carried out, and the free hydrogen contents of samples are presented in Table 4. As shown by the results presented in Table 4, the free hydrogen contents of modified coals were higher than those of raw coal. Moreover, the values of the modified coals increased from 4.79 to 5.36% as the FeS loading increased. This phenomenon indicates that the addition of FeS could introduce more hydrogen into the modified coal during coal hydromodification in a subcritical water−CO system, which improves the hydrogen donation capability of modified coal. This promotes the formation of a developed plastic stage during the pyrolysis of modified coal and increases the caking characteristic of coal. Indeed, the catalytic activity of FeS on coal hydrogenation in a subcritical water−CO system cannot be discussed separately from the synergistic effect of FeS on coal decomposition and the generation of active hydrogen. On one hand, FeS favored the decomposition of coal in subcritical water, which resulted in the generation of a large number of free radicals ($\sum R^{\bullet}$). On the other hand, because of the positive effect that FeS has on free radical's hydrogenation ($\sum R^{\bullet} + H^{\bullet} \rightarrow \sum RH$), the consumption of active hydrogen was accelerated, which induced the forward reaction of WGS to generate more active hydrogen. According to the principles of chemical reaction kinetics, the increased concentrations of $\sum R^{\bullet}$ and active hydrogen were bound to promote the hydrogenation of coal.

In fact, the improvement of the caking characteristic was not only related to the hydrogen content in coal but was also simultaneously influenced by the positions where the active hydrogen was introduced into the caking components. Previous research found that the solutes of Soxhlet extraction were the major caking components in modified coal.[33] Hence, modified coals were separated by Soxhlet extraction, and the extractible solutes were analyzed by ^{1}H NMR. As shown in Figure 5, the yield of each extractible solute in the modified coals was improved compared with that in raw coal. Especially, the extraction yield of TT in the modified coals increases from 15.01 to 38.44% when the FeS loading is raised from 0.0 to 6.0

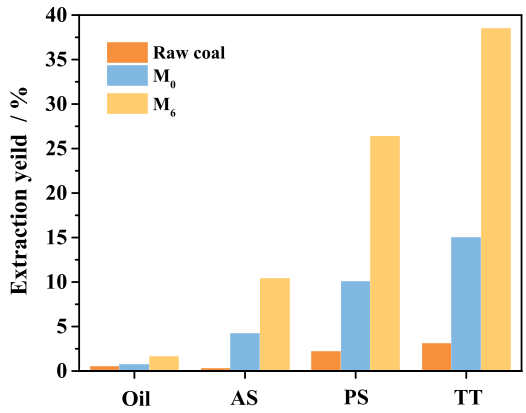

Figure 5. Extraction yields of raw coal and modified coals.

wt %. Comparing the composition of TT between M_0 and M_6, the extraction yields of AS and PS increases from 4.21 and 10.07% to 10.36 and 26.41%, respectively. This is also one of the main reasons for the improvement in the the caking index of M_6.[3,33] Figure 6 presents the ^{1}H NMR spectra of extractible constituents in raw coal and modified coal with/without the FeS catalyst. For all of the curves, aliphatic hydrogens H_{al} (6.0−0.5 ppm) were dominant, whereas the aromatic hydrogens H_{ar} (9.0−6.0 ppm) were weak, indicating that the hydrogen in extractible constituents was mainly associated with the aliphatic carbons or substituents.

Through the integration of ^{1}H NMR spectra, the hydrogen distribution of the samples can be obtained, and the results are presented in Table 5.[34] It can be seen that the ratio of H_{ar} to H_{al} in oil changed little after the hydromodification of coal. This may be because the opening of condensed aromatic rings was accompanied by an increase in the H_{al} content, whereas the cleavage of the branched chains decreased the content of H_{al}. As depicted by the results presented in Table 5, the content of condensed aromatic hydrogen H_c decreased from 1.64 to 0.90, and 0.99%, whereas the content of H_γ decreased from 25.97 to 17.87 and 16.50%, respectively. Compared to the hydrogen distribution of AS in different samples, the ratio H_{ar}/H_{al} increased with the presence of the FeS catalyst than that without the catalyst, indicating that FeS accelerates hydrogen incorporation into the aromatic positions during the formation of AS. In the aliphatic hydrogens of AS, the content of H_α significantly increased with the addition of FeS, whereas the contents of H_β and H_γ decreased rapidly, suggesting that FeS promotes the loss of distal aliphatic side chains and the breakage of methylene bridges between the aromatic rings. As a result, the aromatic rings and $C_{ar}-C_\alpha$ were enriched with a large number of chemical vacancies, leading to the transfer of active hydrogen produced from WGSR into the H_{ar} and H_α positions. Furthermore, because of the cleavage of these branched chains of aromatic rings, the mobility of aromatic rings improved, and the monocyclic aromatic structures were

https://doi.org/10.1021/acsomega.1c03120
ACS Omega 2021, 6, 21160−21168

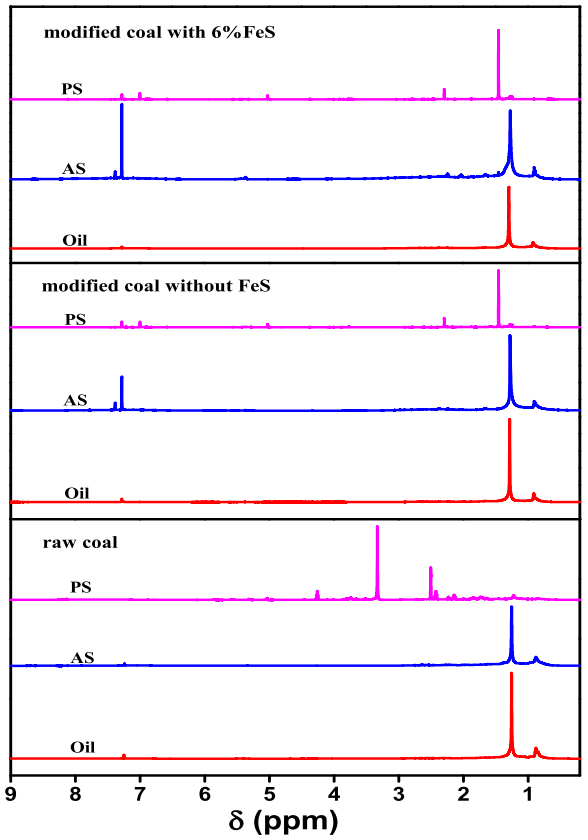

Figure 6. ^{1}H NMR spectra of extractible constituents in raw coal and modified coals.

allowed to rearrange to form polyaromatic units with moderate molecular weights. Consequently, H_c in AS increased from 6.33% in raw coal to 11.92% in modified coal over the FeS catalysts, and this was a larger increase than that achieved with the increment of uncondensed aromatic hydrogen (H_u). However, compared with the hydrogen distribution of PS obtained by catalytic and noncatalytic hydromodification, the FeS catalyst promotes hydrogen into the aliphatic positions instead of aromatic positions during the generation of PS. Moreover, the increase of H_{al} was mainly due to the increase in the fraction of H_β, whereas the decrease of H_{ar} was mainly due to the decrease in the fraction of H_c. This may be because FeS improved the opening of condensed aromatic rings, and the opened longer aliphatic hydrocarbons were more prone to hydrocracking over the FeS catalyst. As a result, the alkyl groups remote from aromatic rings started to break and the content of H_β increased. At the same time, some dissociated alkyl radicals may have been linked to C_α and were stabilized by active hydrogen in the system, which leads to an obvious decrease in the content of H_α in PS.

There is no doubt that the Fe catalyst could accelerate the breakage of the distal alkyl group in the extractible solutes, but the effect on the distribution of H_{ar} in PS is opposite to that in AS. In raw coal, the structures that can be converted into AS and PS may be different. As presented in Table 5, the content of ($H_\beta + H_\gamma$) of AS in raw coal reaches 70.29%, indicating that the long-chain alkanes accounted for a higher proportion. A longer chemical chain is more unstable and hence the chemical chain is more prone to breaking in the presence of the FeS catalyst. When the elimination rate of aromatic vacancies via the condensation became greater than the opening rate of aromatic rings, the H_{ar} content in AS increased. It can be inferred that the FeS catalyst may change the hydrogen distribution of extractible solutes by regulating the hydrocracking reaction.

3.5. Effect of FeS on the Structural Characterization of Modified Coal. *3.5.1. ^{13}C NMR Analysis.* For better understanding the effect of FeS on the carbon skeleton of modified coals, the ^{13}C NMR spectra and the carbon distribution of the samples are shown in Figure 7 and Table 6.[34,35] For all of the curves, the most obvious resonance chemical shift is at 125 ppm, corresponding to the aromatic substituted carbon atom, followed by methylene at ca. 30 ppm and methyl at ca. 20 ppm. Compared to that in raw coal, the aromaticity of M_0 changed little, but the distribution of carbon in aromatic carbon and aliphatic carbon changed greatly. Especially, it is worth noting that the number of methylene groups increases and the content of methyl decreases. The increase in the CH_2/CH_3 ratio indicated that the aliphatic chain linked to aromatic ring in M_0 became longer and the

Table 5. Hydrogen Distribution of Soluble Constituents in Raw Coal and Modified Coals with or without the FeS Catalyst (%)

		oil			AS			PS		
proton type (ppm)	assignments	raw coal	without FeS	with 6.0% FeS	raw coal	without FeS	with 6.0% FeS	raw coal	without FeS	with 6.0% FeS
H_{ar} (9.0−6.0)	aromatic protons	2.02	1.52	2.84	8.50	13.11	17.64	15.27	9.83	8.00
H_c (9.0−7.2)	condensed H_{ar}	1.64	0.90	0.99	6.33	8.22	11.92	10.66	4.09	2.24
H_u (7.2−6.0)	uncondensed H_{ar}	0.38	0.62	1.85	2.17	4.89	5.72	4.62	5.74	5.76
H_{al} (6.0−0.5)	aliphatic protons	97.98	98.48	97.16	91.50	86.89	82.36	84.73	90.17	92.00
H_o (6.0−4.3)	protons of OH, OCHx, and alkenyl of aromatic rings; protons of alkenes	2.91	1.75	1.87	2.54	0.16	4.29	5.93	4.77	4.07
H_α (4.3−2.1)	α position of aromatic rings	7.61	8.85	13.26	11.79	16.21	23.60	44.62	11.87	12.54
H_β (2.1−1.0)	β position of aromatic rings; protons of CH_2 or CH in alkanes	61.49	70.01	65.52	58.50	53.42	46.48	26.92	69.23	71.67
H_γ (1.0−0.5)	γ position of aromatic rings; Protons of CH_3 in alkanes	25.97	17.87	16.50	18.67	17.10	7.99	7.25	4.30	3.72
H_{ar}/H_{al}		0.02	0.02	0.03	0.09	0.15	0.21	0.18	0.11	0.09

https://doi.org/10.1021/acsomega.1c03120
ACS Omega 2021, 6, 21160−21168

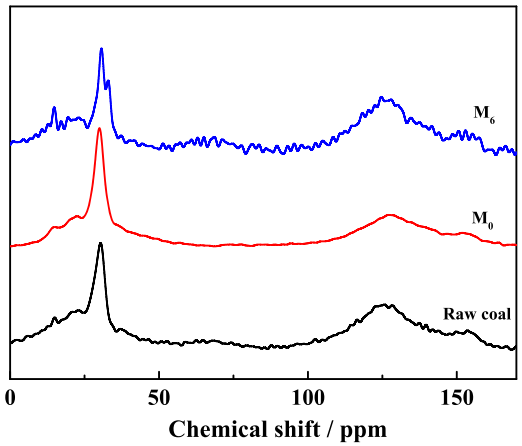

Figure 7. ^{13}C NMR spectra of raw coal and modified coals.

degree of branching decreased. Correspondingly, the content of aromatic carbon connected to aliphatic chains (C_{ar1}) also decreased. By contrast, the aromaticity of M_6 increased significantly, mainly due to the increase of the C_{ar1} content and the decrease of the CH_2 group. This demonstrates that the longer side chains or bridge bonds initially break during the catalytic hydromodification, and then the free radicals with $-CH_2^{\bullet}$ may be stabilized by the active hydrogen in the system, which makes the aliphatic chain shorter. Meanwhile, some of the removed aliphatic chains may be relinked to the aromatic ring to form new chemical bonds, which contributes to the increase in the branching degree of M_6. As shown in Table 6, the content of C_{ar1} increases from 37.75 to 45.37% after the catalytic hydromodification with FeS. Thus, it is certain that FeS would promote the breakage of aliphatic C−H bonds to form the aliphatic structures with shorter chain or higher branched degree, which is conducive to the generation of plastic materials during the coal pyrolysis.[36,37]

3.5.2. XPS Analysis. The results presented in Table 7 show the changes in the amounts of carbon−oxygen forms of raw and modified coals that were obtained from the deconvolution of X-ray photoelectron spectra (Figure 8). The four peaks at 284.8, 285.9, 287.5, and 289.6 eV were assigned to aromatic carbon and aliphatic carbon (C−C/C−H), phenol carbon or ether carbon (C−O), carbonyl (C═O), and carboxyl (COO^-), respectively.[38] As seen in Table 7, the relative amounts of all carbon−oxygen forms in M_0 and M_6 were 27.47 and 23.12%, respectively, which are less than that in the raw coal. Moreover, the hydromodification with 6.0 wt % FeS loading provides a higher decrease in carbon−oxygen forms compared to that without the use of a catalyst. This result is consistent with the elemental analysis of oxygen, as depicted by the results presented in Table 4. It is proposed that the addition of FeS facilitates the removal of oxygen functional groups in a subcritical water−CO system. As a result, the volatile content of modified coals gradually decreased with the addition of FeS, and this can be observed from the results presented in Table 4. In addition, with an increase in the loading of FeS, the decreasing rate of the oxygen form was found in the descending order of COO^- > C═O > C−O. This is due to the poor stability of the carboxyl group, which is most easily removed via FeS-catalyzed pyrolysis and hydrocracking. The C−O form mainly exists in the phenolic hydroxyl and ether bonds. Because the lone pair of electrons of oxygen can be conjugated with the aromatic ring to form a stable structure, it is speculated that the decrease in the relative content of C−O on the surface of modified coal is mainly caused by the breakage of ether bonds. Under the catalytic action of FeS, the removal of oxygen functional groups would reduce the generation of cross-linked bonds during the pyrolysis of modified coal, which is conducive to the transformation of the three-dimensional structure linked by an oxygen bridge bond to the two-dimensional structure. Therefore, the molecular mobility and the caking property of coal would be improved.

Table 7. C 1s and O 1s Analysis of Raw Coal and Modified Coals

			content (ω_{mol} %)		
region	E (eV)	assignment	row coal	M_0	M_6
C 1s	284.8	C−C, C−H	70.00	72.53	76.88
	285.9	C−O	21.22	20.68	18.57
	287.5	C═O	2.07	1.96	1.29
	289.6	COO−	6.71	4.83	3.26
O 1s	530.5	inorg oxygen	1.30	1.18	1.01
	531.7	C═O	20.57	19.56	18.96
	532.8	C−O	62.33	66.24	70.16
	534.0	COO−	13.03	11.73	9.45
	535.4	adsorbed oxygen	2.77	1.29	0.42

4. CONCLUSIONS

The FeS catalyst has a significant catalytic performance on converting the lignite to caking coal in a subcritical water−CO system, whereas the caking index (G_{RI}) of the modified coal reaches the maximum value of 95 for the FeS loading of 6.0 wt %. The major function of FeS catalysts on the hydromodification is to synergistically promote the conversion of CO and the pyrolysis and hydrogenation of coal. FeS promotes the decomposition of coal in subcritical water to generate free

Table 6. Carbon Distribution of Raw Coal and Modified Coals (%)

		molar content (%)		
carbon type (ppm)	assignments	raw coal	M_0	M_6
C_{ar} (165−90)	aromatic carbons	44.26	45.74	50.37
C_{ar1} (165−120)	aromatic carbons connected to aliphatic chains, heteroatomic or aromatic substituents, and condensed aromatic rings shared by two rings	37.75	36.00	45.37
C_{ar2} (120−90)	aromatic carbons of condensed aromatic rings shared by three rings; protonated aromatic carbons	6.51	9.74	5.00
C_{al} (50−0)	aliphatic carbons	55.74	54.26	49.63
CH_2 (50−25)	methylene; methine	34.55	38.96	28.29
CH_3 (25−0)	methyl	21.19	15.30	21.34
$f_a = C_{ar}/C_{total}$		0.44	0.46	0.50

https://doi.org/10.1021/acsomega.1c03120
ACS Omega 2021, 6, 21160−21168

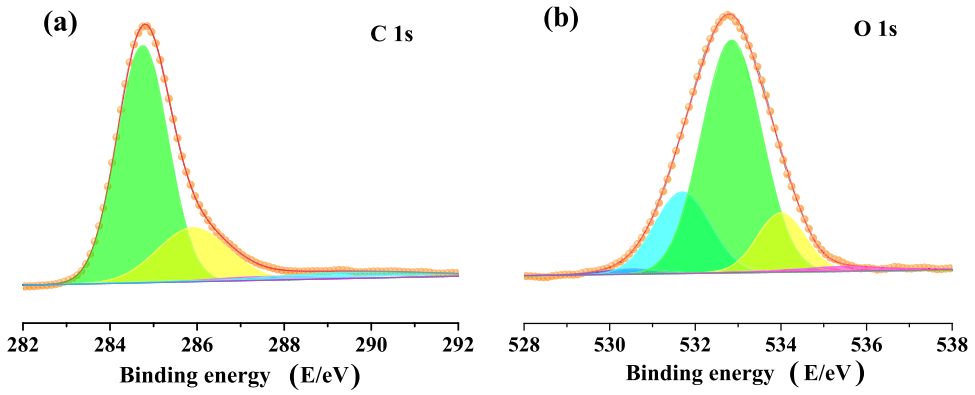

Figure 8. Deconvoluted X-ray photoelectron spectra for C 1s (a) and O 1s (b).

radicals and accelerates the production and incorporation of active hydrogen from WGSR into modified coal, which facilitates the forward water gas shift reaction to increase X_{CO} and provide more H$^{\bullet}$ for the hydromodification of coal. In the presence of FeS, the hydromodification of lignite would lead to the breakage of distal aliphatic C−H bonds in the extractible solutes, which promotes the entrance of hydrogen into H_{β} of PS and H_{ar} and H_{α} of AS. The generation of an aliphatic structure with a shorter chain and a higher degree of branched chain is conducive to the formation of plasticity in the process of coal pyrolysis. In addition, the addition of FeS would enhance the deoxygenation of coal along with the reduction of volatiles, thereby improving the caking property characteristic of modified coal.

AUTHOR INFORMATION

Corresponding Authors

Yuqiong Zhao − *State Key Laboratory of Clean and Efficient Coal Utilization, Taiyuan University of Technology, Taiyuan 030024, China*; orcid.org/0000-0003-2858-0580; Email: muye0925@163.com

Yongfa Zhang − *State Key Laboratory of Clean and Efficient Coal Utilization, Taiyuan University of Technology, Taiyuan 030024, China*; Email: yongfaz@tyut.edu.cn

Authors

Shouqi He − *State Key Laboratory of Clean and Efficient Coal Utilization, Taiyuan University of Technology, Taiyuan 030024, China*

Qingxiang Guo − *State Key Laboratory of Clean and Efficient Coal Utilization, Taiyuan University of Technology, Taiyuan 030024, China*

Guoqiang Li − *State Key Laboratory of Clean and Efficient Coal Utilization, Taiyuan University of Technology, Taiyuan 030024, China*

Liping Wang − *Shanxi Guoxin Gas Energy Institute Co., Ltd., Taiyuan 030024, China*

Yunbo Liu − *College of Chemistry and Chemical Engineering, Taiyuan University of Technology, Taiyuan 030024, China*

Complete contact information is available at: https://pubs.acs.org/10.1021/acsomega.1c03120

Notes

The authors declare no competing financial interest.

ACKNOWLEDGMENTS

This work was supported by the National Natural Science Foundation of China (21805203 and 21576182), the 2020 Shanxi Provincial Postgraduate Innovation Program (2020SY540), and the 2020 Shanxi Provincial College Students Innovation Program (2020100).

REFERENCES

(1) Wang, M. J.; Wang, Q.; Li, T.; Kong, J.; Shen, Y. F.; Chang, L. P.; Xie, W.; Bao, W. R. Catalytic upgrading of coal pyrolysis volatiles by porous carbon materials derived from the blend of biochar and coal. *ACS Omega* **2021**, *6*, 3800−3808.

(2) Liu, P.; Zhang, D. Effect of hydrothermal treatment on the carbon structure of Inner Mongolia lignite. *Int. J. Coal Sci. Technol.* **2020**, *7*, 493−503.

(3) Zhao, Y.; Zhang, M.; Cui, X. T.; Dong, D. L.; Wang, Q.; Zhang, Y. F. Converting lignite to caking coal via hydro-modification in a subcritical water-CO system. *Fuel* **2015**, *167*, 1−8.

(4) Nandi, B. N.; Ternan, M.; Belinko, K. Conversion of non-coking coals to coking coals by thermal hydrogenation. *Fuel* **1981**, *60*, 347−354.

(5) Shui, H. F.; Zhang, X. Y.; Wang, Z. C.; Lin, C. H.; Lei, Z. P.; Ren, S. B.; Kang, S. G. Modification of a Sub-bituminous Coal by Hydrothermal Treatment with the Addition of CaO: Extraction and Caking Properties. *Energy Fuels* **2012**, *26*, 2928−2933.

(6) He, S. Q.; Zhao, Y. Q.; Zhang, Y. F.; Wang, Q. Structural Evolution of Group Components and Caking Change for Hydro-modifed Lignite. *Coal Convers.* **2021**, *44*, 9−17.

(7) Liu, X. C.; Ling, Q.; Zhao, Z. G.; Xie, R. L.; Yu, D. L.; Ke, Q. P.; Lei, Z.; Cui, P. Effects of low-temperature rapid pyrolysis treatment on the improvement in caking property of a chinese sub-bituminous coal. *J. Anal. Appl. Pyrolysis* **2018**, *135*, 319−326.

(8) Saikia, B. K.; Boruah, R. K.; Gogoi, P. K.; Baruah, B. P. A thermal investigation on coals from Assam (India). *Fuel Process. Technol.* **2009**, *90*, 196−203.

(9) Laggoun-Défarge, F.; Rouzaud, J. N.; Iglesias, M. J.; Isabel, S. R.; Nicolas, B.; et al. Coking properties of perhydrous low-rank vitrains. Influence of pyrolysis conditions. *J. Anal. Appl. Pyrolysis.* **2003**, *67*, 263−276.

(10) Wang, Z. C.; Shui, H. F.; Pei, Z. N.; Gao, J. S. Study on the hydrothermal treatment of Shenhua coal. *Fuel* **2008**, *87*, 527−533.

(11) Racovalis, L.; Hobday, M. D.; Hodges, S. Effect of processing conditions on organics in wastewater from hydrothermal dewatering of low-rank coal. *Fuel* **2002**, *81*, 1369−1378.

(12) Huang, P.; Du, M. H.; Li, K. J. Study on the caking improvement of Shenhua coal by hydrogenation. *J. China Coal Soc.* **2009**, *34*, 683−687.

(13) Dong, D. L.; Zhang, Y. F.; Zhao, Y. Q.; Wang, Q. Improvement in the Caking Property of Lignite by Hydromodification in a CO Subcritical Water System. *Chem. Lett.* **2014**, *43*, 1470−1472.
(14) Wang, D. S.; Huang, P.; Bai, X. F. Experiment research on low metamorphic bituminous coal hydrogenated to improve plasticity and quality. *Coal Sci. Technol.* **2008**, *36*, 104−106.
(15) Zhang, Y.; Wang, L. P.; Tuo, K. Y.; Liu, S. Q. Microwave-assisted pyrolysis of low-rank coal with K_2CO_3, $CaCl_2$, and $FeSO_4$ Catalysts. *ACS Omega* **2020**, *5*, 17232−17241.
(16) Feng, J.; Xue, X. Y.; Li, X. H.; Li, W. Y.; Guo, X. F.; Liu, K. Products analysis of shendong long-flame coal hydropyrolysis with iron-based catalysts. *Fuel Process. Technol.* **2015**, *130*, 96−100.
(17) Ali, A.; Zhao, C. Direct liquefaction techniques on lignite coal: A review. *Chin. J. Catal.* **2020**, *41*, 375−389.
(18) Borah, D.; Barua, M.; Baruah, M. K. Dependence of pyrite concentration on kinetics and thermodynamics of coal pyrolysis in nonisothermal systems. *Fuel Process. Technol.* **2005**, *86*, 977−993.
(19) Kabe, T.; Saito, M.; Qian, W.; Ishihara, A. Elucidation of hydrogen mobility in coal using a tritium pulse tracer method. Hydrogen exchange reaction of coal with tritiated gaseous hydrogen. *Fuel* **2000**, *79*, 311−316.
(20) Ishihara, A.; Nishigori, D.; Saito, M.; Sturisna, I. P.; Qian, W.; Kabe, T. Elucidation of hydrogen mobility in functional groups of coals using tritium tracer methods. *Energy Fuels* **2002**, *16*, 32−39.
(21) Li, X.; Hu, S. X.; Jin, L. J.; Hu, H. Q. Role of iron-based catalyst and hydrogen transfer in direct coal liquefaction. *Energy Fuels* **2008**, *22*, 1126−1129.
(22) Niu, B.; Jin, L. J.; Li, Y.; Shi, Z. W.; Hu, H. Q. Isotope analysis for understanding the hydrogen transfer mechanism indirect liquefaction of Bulianta coal. *Fuel* **2017**, *203*, 82−89.
(23) Artanto, Y.; Jackson, W. R.; Redlicha, P. J.; Marshalla, M. Liquefaction studies of some Indonesian low rank coals. *Fuel* **2000**, *79*, 1333−1340.
(24) Li, H.; Wu, S. Y.; Wu, Y. Q.; Huang, S.; Gao, J. S. A preliminary investigation of CO effects on lignite liquefaction process. *Fuel* **2018**, *221*, 417−424.
(25) Li, H.; You, Q.; Wu, S. Y.; Wu, Y. Q.; Huang, S.; Gao, J. S. Characteristics of Na_2CO_3-catalyzed water-gas shift reaction under coal liquefaction conditions. *Fuel* **2018**, *232*, 639−644.
(26) Li, L.; Huang, S.; Wu, S. Y.; Wu, Y. Q.; Gao, J. S. Roles of Na_2CO_3 in lignite hydroliquefaction with Fe-based catalyst. *Fuel Process. Technol.* **2015**, *138*, 109−115.
(27) Xu, Y.; Zhang, D. X.; Jin, S.; Zhao, A. A.; Gao, J. S. Study on Shengli brown coal liquefaction in CO+H_2O system. *Chem. Eng.* **2010**, *38*, 95−98.
(28) Wang, Q.; Zhao, Y. Q.; Zhang, Y. F.; Zhang, T. K.; He, S. Q.; Wei, Y. Isotope labeling to study the hydrogen transfer route during lignite modification in subcritical D_2O-CO system. *Energy Fuels* **2020**, *34*, 5485−5496.
(29) Zhao, Y.; Guo, Y. F.; Zhang, H. R.; Zhang, Y. F.; Wang, Q. Structural characterization of carbonized briquette obtained from anthracite powder. *J. Anal. Appl. Pyrolysis* **2015**, *112*, 290−297.
(30) Siskin, M.; Katritzky, A. R. Reactivity of organic compounds in hot water: geochemical and technological implications. *Science* **1991**, *254*, 231−237.
(31) Ouchi, K.; Makabe, M. Hydrogen transfer in the hydrogenation of model compounds. *Fuel* **1988**, *67*, 1536−1541.
(32) Xie, K. C. *Coal Structure and Its Reactivity*; Science Press: Beijing, 2002.
(33) Wang, Q.; Zhang, T. K.; Zhao, Y. Q.; He, S. Q.; Zhang, Y. F. Structural evolution and formation mechanisms of caking components of modified lignite in subcritical H_2O-CO systems. *Energy Fuels* **2019**, *33*, 12073−12082.
(34) Wang, M. Y.; Jin, L. J.; Li, Y.; Lv, J. N.; Wei, B. Y.; Hu, H. Q. In-situ catalytic upgrading of coal pyrolysis tar coupled with CO_2 reforming of methane over Ni-based catalysts. *Fuel Process. Technol.* **2018**, *177*, 119−128.
(35) Alhumaidan, F. S.; Hauser, A.; Rana, M. S.; Lababidi, H. M. NMR characterization of asphaltene derived from residual oils and their thermal decomposition. *Energy Fuels* **2017**, *31*, 3812−3820.
(36) Li, X.; Qin, Z. H.; Bu, L. H.; Yang, Z.; Shen, C. Y. Structural analysis of functional group and mechanism investigation of caking property of coking coal. *Fuel Chem. Technol.* **2016**, *44*, 385−393.
(37) Hui, Y. Z.; Tian, L.; Lee, S.; Chen, Y. X.; Tahmasebi, A.; Mahoney, M.; Yu, J. L. A comprehensive study on the transformation of chemical structures in the plastic layers during coking of Australian coals. *J. Anal. Appl. Pyrolysis.* **2020**, *152*, 104947.1−104947.10.
(38) Kelemen, S. R.; Afeworki, M.; Gorbaty, M. L.; Cohen, A. D. Characterization of organically bound oxygen forms in lignites, peats, and pyrolyzed peats by X-ray photoelectron spectroscopy (XPS) and solid-state ^{13}C NMR methods. *Energy Fuels* **2002**, *16*, 1450−1462.

https://doi.org/10.1021/acsomega.1c03120
ACS Omega 2021, 6, 21160−21168